Vol. 06, No. 4 (2024) 1787-1792, doi: 10.24874/PES.SI.25.03b.001

Proceedings on Engineering Sciences

www.pesjournal.net

DIELECTRIC STUDIES ON TSP: $NANO_3$ BIOPOLYMER-BASED POLYMER ELECTROLYTES

M. Gnana Kiran[1]
Sharmila. D
Rao. M. C
Naveen Kumar. V
Krishna Jyothi. N

Received 31.10.2023.
Received in revised form 29.12.2023.
Accepted 12.02.2024.
UDC – 537.226.2

Keywords:

TSP, $NaNO_3$, Conductivity, Impedance Analysis, Dielectric Constant

A B S T R A C T

The solution cast method made free-standing tamarind seed polysaccharide (TSP): Sodium Nitrate ($NaNO_3$) based solid polymer electrolyte films with various weight percentages. The conductance and dielectric properties of the polymer films were evaluated using AC impedance spectroscopy. This polymer electrolyte's conductance varied with temperature. By raising the temperature for different concentrations, the conductivity was increased. The maximum conductivity was obtained for 70:30 films at 373 K. According to dielectric studies, dielectric constants and dielectric loss were higher at low frequencies and lower at higher frequencies. At 303 K, the dielectric constant (ε^1) was 899.1, and the dielectric loss (ε^{11}) was 1393.8 for 70:30 (TSP: $NaNO_3$) composition. The minimal tangent loss was 1.54×10^{-4} for 30% film.

1. INTRODUCTION

Solid biopolymer electrolytes (SBPE) are a thrust area compared to other research domains. There are several benefits to using these electrolytes. These material samples can be easily prepared in a lab. Solid polymer electrolytes are mechanically strong, offer more conductivity, and have less leakage (Singh et al., 2016). Over the past few decades, substantial research has been carried out on electrolytes using synthetic polymers (Raju et al. 2019). These polymers, therefore, take a very long time to decompose.

Consequently, biopolymers overcome the issue above (Park et al., 2003). Proteins, polyesters, and polysaccharides are the three subcategories of biopolymers. Pectin, starch, agar-agar, cellulose, chitosan, and agarose are some such polysaccharides (Kulkarni et al., 2021) Polysaccharide-based biopolymers are extremely useful in electrochemical devices since they are eco-friendly, quickly degrading materials. Tamarind Seed Polysaccharide (TSP) is a special biopolymer with outstanding properties and uses. For example, effective gelling agents, simple film-forming abilities, etc. A lot of polar groups are present in this highly branched polysaccharide. 3:1:2 molar ratios of glucose, galactose, and xylose sugar monomers can be

[1] Corresponding author: Gnana Kiran. M,
Email: gnanakiran33@gmail.com

found in TSP (Saha et al., 2023). Numerous applications of TSP have been the subject of substantial research. Recent studies on TSP for various medicine formulations have shown other distinctive properties, such as its potent antidiabetic activity (Bharathi et al., 2023), which decreases blood sugar levels. It is also an excellent excipient for ocular preparations because of its capacity to create flexible films with high tensile strength.

The characteristics of this film include transparency, non-hygroscopicity, non-stickiness, shape preservation even after harsh handling, and ferning patterns like those of natural tear film (Basha et al., 2017). TSP works as a binder, thickener, stabilizer, and good gelling agent. It increases viscosity in various industries, including cosmetics, food packaging, medicine, and numerous drug products (Rambabu et al., 2023). At 60 to 80 ^{o}C, it can only be completely resolved in inorganic liquids like water. Only a few research have been reported on TSP biopolymers until now. Fig. 1 represents the molecular structure of TSP (Selvakumar & Bhat, 2008). This research prepares a biopolymer electrolyte by adding biopolymer TSP with dopant salt $NaNO_3$ for various concentrations of dopant salt $NaNO_3$ by solution cast procedure in laboratory methods. AC impedance spectroscopy allows it to observe electrical conductivity studies and dielectric properties (Vijaya et al., 2017, Pandi et al., 2016).

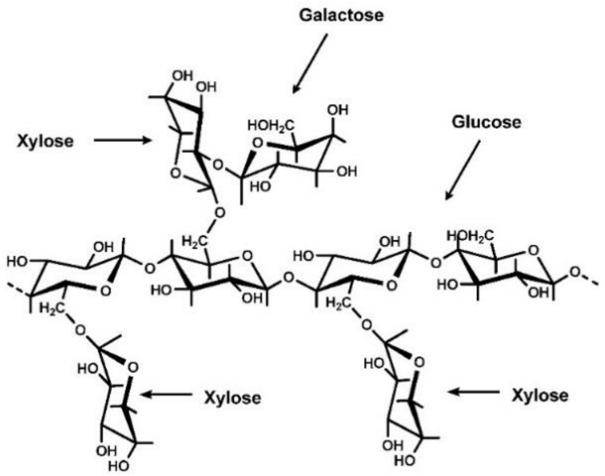

Figure 1. Molecular Structure of Tamarind Seed Polysaccharides

2. MATERIAL AND METHODS

TSP is purchased from Tokyo Chemical Industries (TCI) in Japan. The solid biopolymer electrolyte films were made using the solution cast technique in this study. TSP is dissolved in double-distilled water (H_2O) with $NaNO_3$ added in the compositional ratios of (90:10), (80:20), (70:30), and (60:40), and the mixture is stirred for 12 hours at a temperature of 60 ^{o}C using magnetic stirrers. After forming a very homogeneous and viscous solution, transparent or partially transparent thin films ranging from 0.08 to 0.11 mm are generated after 24 h when the mixture is poured into Petri dishes and deposited in a vacuum chamber with the temperature kept at 60 ^{o}C. A computer equipped HIOKI 3532 LCR testing meter measures solid biopolymer electrolyte's electrical and ionic conductivity properties at 42 to 1 MHz temperatures.

3. RESULTS AND DISCUSSIONS

3.1 Conductivity Studies

The electrical relaxations in AC frequency are split into three states. In the first state, high-frequency electrical relaxations are correlated with short-range ion movement (Majid et al., 2005). In second-state middle frequencies, the relaxations are associated with the long-range direction of ions. Dopants, point defects, and grain boundaries influence the relaxations. At a lower frequency, the relaxation is assigned to charge transfer. Third low region, asymmetric plots that gradually increase from a lower end to a higher end are due to ions moment and charge carrier concentrations (Premalatha et al., 2017). The conductance of ions is defined by the density and flow rate (Kiran et al., 2019).

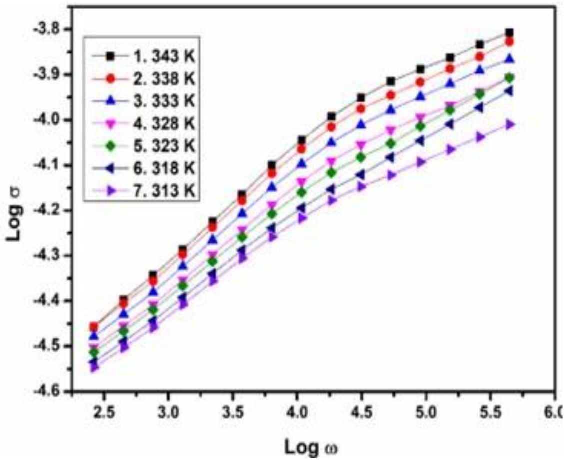

Figure 2. Conductance plot between Log ω vs. Log σ at various temperatures for 30% film

Fig. 2 is drawn between 'Log ω' and 'Log σ'. Here by raising the temperature, conductance increases gradually with respect to frequency. This plot shows two different regions; one is a low-frequency region and another one is a high-frequency region. At the first low region, all plots look merged and overlapped. At high-frequency regions, conductance increases by increasing the temperature and frequency (Premalatha et al., 2016). Here, the conductance is increased due to the migration of ions.

3.2 Conductivity vs. Composition

Fig. 3 shows the plot between the composition concentration and conductivity of the materials at different temperatures. Pure TSP and TSP with a salt of various concentrations are taken in this composition. By increasing the temperature of each composition, the conductivity is also increased gradually. Initially, the conductivity is very low for pure TSP at room temperature. By raising the temperature for different concentrations, the conductivity is increased. Finally, the maximum conductivity is obtained for 70:30 film at 373 K., Yet the conductivity decreases by raising the salt concentration to the polymer. The conductivity change can be observed as shown in the given plots with respect to temperature. The conductivity is raised due to the migration and movement of ions through the material (Hamsan et al., 2020).

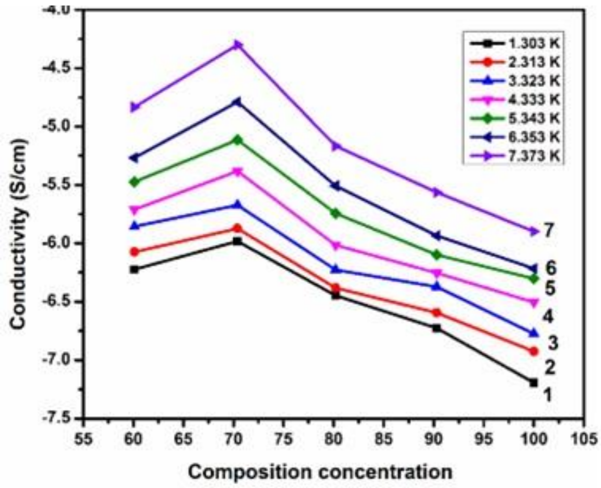

Figure 3. Composition Concentration vs. Conductivity plot for various wt.% ratios of TSP: $NaNO_3$

Due to the movement of ions in the polymer material, the polymer chain segments are increased, which finally causes the conductivity of the ions (Jyothi et al., 2022). At various temperatures, plots were drawn between the Conductivity and Composition of the films (Fig. 3). For a particular film composition, the conductivity progressively increases as the temperature is enhanced (Ma et al., 2007). At a specific temperature, the conductivity increases as the percentage of $NaNO_3$ increases to 30%. Then onwards, again, the conductivity decreased.

3.3 Dielectric Properties

The dielectric parameters are measured from the electrical properties of pure and doped films. Fig. 4 and 5 show the frequency dependence of ε^1 and ε^{11}. At low frequencies, ε^1 and ε^{11} are higher. As the frequency increases, the values decrease gradually and remain constant at high frequencies (Sikkanthar et al., 2015). The decrease in dielectric constant and dielectric energy loss for ions at high frequencies may be due to the space charge effect and polarization (Kiran et al., 2021). Moreover, it can be deduced from the graphs that the 30% film has demonstrated the largest dielectric constant (ε^1) and dielectric loss (ε^{11}).

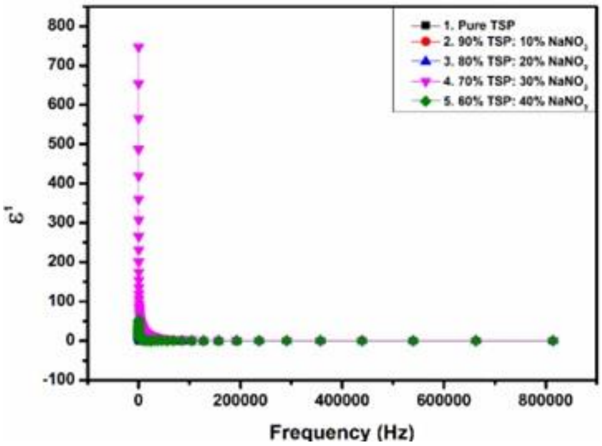

Figure 4. Dielectric plot between frequency vs. ε^1 for TSP: $NaNO_3$ at various wt.% ratios

The information is displayed in Table 1. The parameters are decreased with a decrease in salinity or an increase in salinity (Gnana Kiran et al. 2023). For pure TSP, the computed permittivity (dielectric constant) is 14.4. However, the dielectric permittivity of TSP films with 10%, 20%, and 30% $NaNO_3$ doping is 30.0, 42.7, and 899.1, respectively. However, the dielectric constant is once more reduced to 62.2 with a 40% doped layer. Similar to this, pure TSP has a dielectric loss of 34.2. However, the dielectric losses for 10%, 20%, and 30% $NaNO_3$ doped TSP films are 64.6, 67.1, and 1393.8, respectively. Again, the dielectric loss is reduced to 134.8 in a 40% doped layer. The 30% film has a higher dielectric constant and dielectric loss than the other films because it is more conductive and amorphous (Mishra & Khandare, 2011).

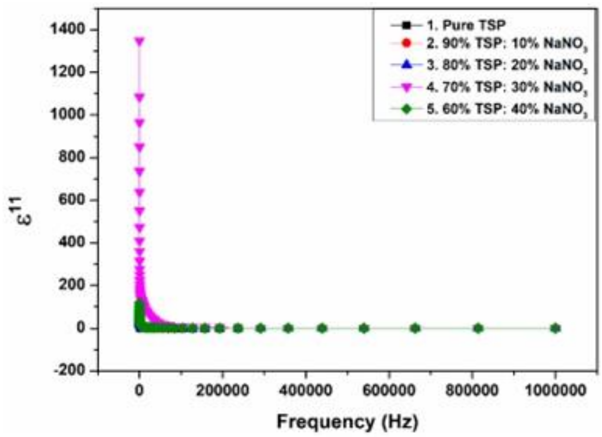

Figure 5. Dielectric plot between frequency vs. ε^{11} for TSP: $NaNO_3$ at various wt.% ratios

The relation time may be responsible for these differences in the parameters. At low frequencies, the electric dipoles have enough time to align themselves in the field's direction (Armstrong et al., 1972). However, at high-frequency ranges, the dipoles cannot spend enough time aligning themselves with the field direction, which results in a low dielectric constant and dielectric loss (Marzantowicz et al., 2007).

Table 1. Dielectric constant and dielectric loss of TSP: $NaNO_3$ at various wt.% ratios

S. No	Composition wt. % (TSP: $NaNO_3$)	ε^1	ε^{11}
1	Pure TSP	14.4	34.2
2	90: 10	30.0	64.6
3	80: 20	42.7	67.1
4	70: 30	899.1	1393.8
5	60: 40	62.2	134.8

3.4 Tangent loss

Fig. 6 is drawn between 'Log ω' and tangent loss (Tan δ) of pure TSP and TSP with various wt.% ratios of the salt. The tangent loss represents the total energy loss in the system. And it is the ratio between dielectric energy loss and dielectric constant ($\varepsilon^{11}/\varepsilon^1$). The peak maximum indicates energy loss (Adachi & Urakawa, 2002). It may be inferred from the plot that with pure TSP, energy loss is more than in other composite films. The data is presented in Table 2. The calculated tangent loss for pure TSP is $2.34x10^{-4}$. But with 10%, 20%, and 30% $NaNO_3$ doped TSP films, the tangent energy losses are $2.26x10^{-4}$, $2.12x10^{-4}$, and $1.54x10^{-4}$, respectively. But with 40% doped film, the tangent energy loss again increases to $1.72x10^{-4}$. The tangent loss is obtained by the fallowing farmula,

$$\text{Tan } \delta = \frac{\varepsilon^{11}}{\varepsilon^{1}} \quad (1)$$

Table 2. Tangent loss of TSP: $NaNO_3$ at various wt.% ratios

S. No	Composition wt. % (TSP: $NaNO_3$)	Tan δ
1	Pure TSP	2.34×10^{-4}
2	90: 10	2.26×10^{-4}
3	80: 20	2.12×10^{-4}
4	70: 30	1.54×10^{-4}
5	60: 40	1.72×10^{-4}

As the salt concentration is increased in the host material from 10% to 30%, tangent energy losses are decreased gradually. The lowest energy loss is observed with 30% film. Further increasing the dopant concentration up to 40% increases the tangent energy loss. The tangent loss is evaluated as per equation (Jyothi et al., 2022).

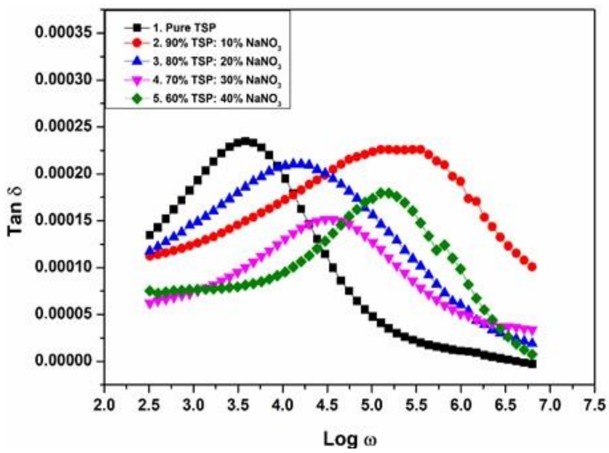

Figure 6. Tangent loss plot of TSP: $NaNO_3$ at various wt.% ratios

4. CONCLUSION

This study uses the solution cast method to examine synthesized TSP-based polymer electrolyte membranes with different $NaNO_3$ concentrations (10, 20, 30, and 40%). Electrical features, including conductance analysis, dielectric properties, tangent loss, and electrical modulus, are assessed for the films at various compositions to characterize them. By raising the temperature for different concentrations, the conductivity is increased. The maximum conductivity is obtained for 70:30 films at 373 K. Furthermore, the dielectric measurements show that the "dielectric constant" and "dielectric losses" are maxima for 30% film: 899.1 and 1393.8, respectively. The tangent energy loss is minimum for 30% film and is $1.54x10^{-4}$.

Acknowledgement: Thanks to the Department of Science and Technology (DST, Delhi), Government of India, for providing the Department of Physics with the DST-FIRST Level-1 (SR/FST/PS-1/2018/35) initiative. We thank the KLEF for providing the facilities, infrastructure, basic instruments, and assistance for the current project.

References:

Adachi, K., & Urakawa, O. (2002). Dielectric study of concentration fluctuations in concentrated polymer solutions. *Journal of non-crystalline solids*, *307*, 667-670. doi:10.1016/S0022-3093(02)01527-2

Armstrong, R. D., Dickinson, T., & Whitfield, R. (1972). The impedance of the silver-solid electrolyte interphase. *Journal of Electroanalytical Chemistry and Interfacial Electrochemistry*, *39*(2), 257-262. https://doi.org/10.1016/S0022-0728(72)80150-5

Basha, S. S., Gnanakiran, M., Ranjit Kumar, B., Veera Bhadra, K., Reddy, M., & Rao, M. (2017). Synthesis and spectral characterization on PVA/PVP: GO based blend polymer electrolytes. *Rasayan Journal of Chemistry, 10*, 1159-1166. http://dx.doi.org/10.7324/RJC.2017.1041756

Bharathi, R. V., Raju, M. K., Shanmukhi, P. S. V., Kiran, M. G., Murali, N., Parajuli, D., & Samatha, K. (2023). Enhanced DC electrical resistivity and magnetic properties of transition metal cobalt substituted spinel MgFe2O4 ferrite system. *Inorganic Chemistry Communications*, 111713. doi:10.1016/j.inoche.2023.111713

Gnana Kiran, M., Jyothi, N. K., Rao, M. C., Babu, S. K., Pardhasaradhi, P., Prasad, G. R. K., Rao, M. P., & Samatha, K. (2023). Structural, electrical, and dielectric studies of PVA-based NaNO3 polymer electrolytes for battery applications. *International Journal of Ambient Energy, 44*(1), 246-255. doi: 10.1080/01430750.2022.2126521

Hamsan, M. H., Aziz, S. B., Nofal, M. M., Brza, M. A., Abdulwahid, R. T., Hadi, J. M., ... & Kadir, M. F. Z. (2020). Characteristics of EDLC device fabricated from plasticized chitosan: MgCl2 based polymer electrolyte. *Journal of Materials Research and Technology*, *9*(5), 10635-10646. doi:10.1016/j.jmrt.2020.07.096

Jyothi, N., Krishna, K., Rao, K. T., Kumar, V. N., Gnana Kiran, M., Deepthi, K., Rao, M. C., Kumar, K. V., & Inthiyaz, S. (2022). Synthesis and dielectric properties of PAN-based Na+ ion polymer electrolytes. *Materials Today: Proceedings*, *51*, 1168-1171. doi:10.1016/j.matpr.2021.07.123

Jyothi, N., Krishna, M. Gnana Kiran, Kumar, V. N., Rao, B. N., Kumar, K. V., & Rao, M. C. (2022). Structural and impedance analysis of PAN-based Na+ ion conducting gel polymer electrolytes for energy storage device application. *Materials Today: Proceedings, 51*, 1164-1167. doi:10.1016/j.matpr.2021.07.122

Kiran, M. Gnana, Jyothi, N. K., Samatha, K., Rao, M. P., & Prasad, V. B. V. N. (2021). Studies on optical properties of PVA-based complex polymer electrolyte. *RASAYAN Journal of Chemistry, 14*, 760-767. http://dx.doi.org/10.31788/RJC.2021.1425964

Kiran, M. Gnana, Jyothi, N. K., Rao, M. N., & Kumar, K. V. (2019). AC conductivity and dielectric studies of PVA-based solid polymer electrolyte. *Journal of the Indian Chemical Society, 96*(1), 76-77.

Kulkarni, G. T., Paritala, S., & Siddaiah, M. K. (2011). Effect of tamarind seed polysaccharide on dissolution behaviour of ibuprofen tablets. *Journal of Chronotherapy & Drug Delivery, 2*, 49-56.

Ma, X., Yu, J., He, K., & Wang, N. (2007). The effects of different plasticizers on the properties of thermoplastic starch as solid polymer electrolytes. *Macromolecular Materials and Engineering*, *292*(4), 503-510. doi:10.1002/mame.200600445

Majid, S. R., & Arof, A. K. (2005). Proton-conducting polymer electrolyte films based on chitosan acetate complexed with NH4NO3 salt. *Physica B: Condensed Matter, 355*(1-4), 78-82. doi:10.1016/j.physb.2004.10.025

Marzantowicz, M., Dygas, J. R., Krok, F., Florjańczyk, Z., & Zygadło-Monikowska, E. (2007). Influence of crystalline complexes on electrical properties of PEO: LiTFSI electrolyte. *Electrochimica Acta, 53*(4), 1518-1526. doi:10.1016/j.electacta.2007.03.032

Mishra, M. U., & Khandare, J. N. (2011). Evaluation of tamarind seed polysaccharide as a biodegradable carrier for colon-specific drug delivery. *International Journal of Pharmacy and Pharmaceutical Sciences, 3*(1), 139-142.

Pandi, D. V., Selvasekarapandian, S., Bhuvaneswari, M., Premalatha, S., Monisha, D., Arunkumar, & Junichi, K. (2016). Development and characterization of proton conducting polymer electrolyte based on PVA, amino acid glycine, and NH4SCN. *Solid State Ionics*, *298*, 15-22. doi:10.1016/j.ssi.2016.10.016

Park, C. H., Kim, D. W., Prakash, J., & Sun, Y. K. (2003). Electrochemical stability and conductivity enhancement of composite polymer electrolytes. *Solid State Ionics, 159*(1-2), 111-119. doi: 10.1016/S0167-2738(03)00025-0

Premalatha, M., Mathavan, T., Selvasekarapandian, S., Monisha, S., Vinoth Pandi, D., & Selvalakshmi, S. (2016). Investigations on proton conducting biopolymer membranes based on tamarind seed polysaccharide incorporated with ammonium thiocyanate. *Journal of Non-Crystalline Solids, 453*, 131-140. doi:10.1016/j.jnoncrysol.2016.10.008

Premalatha, M., Mathavan, T., Selvasekarapandian, S., Monisha, S., Selvalakshmi, S., & Vinoth Pandi, D. (2017). Tamarind seed polysaccharide (TSP)-based Li-ion conducting membranes. *Ionics, 23*, 2677-2684. doi:10.1007/s11581-017-1989-x

Raju, G., Murali, N., Prasad, M. S. N. A., Suresh, B., Babu, D. A., Kiran, M. Gnana, Ramakrishna, A., Tulu, W. M., & Kishore, B. (2019). Effect of chromium substitution on the structural and magnetic properties of cobalt ferrite. *Materials Science for Energy Technologies, 2*(1), 78-82. doi:10.1016/j.mset.2018.11.001

Rambabu, C., Aruna, B., Shanmukhi, P. S. V., Kiran, M. G., Murali, N., Mammo, T. W., & Narayana, P. L. (2023). Effect of La3+/Cu2+ and La3/Ni2+ substitution on the synthesis, magnetic and dielectric properties of M− type Sr1-xLaxFe12-xMxO19 (M= Cu and Ni) hexaferrite. *Inorganic Chemistry Communications*, 111753. doi:10.1016/j.inoche.2023.111753

Saha, A., Kumar, K. V., Jyothi, N. K., Kiran, M. G., & Rao, M. C. (2023). Structural and electrical properties of TSP: CH3COONa amorphous biopolymer electrolytes for electrochemical cell applications. *Journal of Non-Crystalline Solids, 616*, 122465. doi:10.1016/j.jnoncrysol.2023.122465

Selvakumar, M., & Bhat, D. K. (2008). LiClO4 doped cellulose acetate as biodegradable polymer electrolyte for supercapacitors. *Journal of Applied Polymer Science, 110*(1), 594-602.

Sikkanthar, S., Karthikeyan, S., Selvasekarapandian, S., Vinoth Pandi, D., Nithya, S., & Sanjeeviraja, C. (2015). Electrical conductivity characterization of polyacrylonitrile-ammonium bromide polymer electrolyte system. *Journal of Solid-State Electrochemistry*, *19*(5), 987-999. doi:10.1007/s10008-014-2697-3

Singh, R., Polu, A. R., Bhattacharya, B., Rhee, H. W., Varlikli, C., & Singh, P. K. (2016). Perspectives for solid biopolymer electrolytes in dye-sensitized solar cell and battery application. *Renewable and Sustainable Energy Reviews*, *65*, 1098-1117. doi:10.1016/j.rser.2016.06.026

Vijaya, N., Selvasekarapandian, S., Sornalatha, M., Sujithra, K. S., & Monisha, S. (2017). Proton-conducting biopolymer electrolytes based on pectin doped with NH4X (X= Cl, Br). *Ionics*, *23*(10), 2799-2808. doi:10.1007/s11581-016-1852-5

M. Gnana Kiran
Department of Engineering Physics,
KLEF, Vaddeswaram,
Andhra Pradesh,
India
gnanakiran33@gmail.com
ORCID 0000-0002-1465-5265

Sharmila. D
Dept. of. E&IT,
Aacharya Nagarjuna University,
Nambur, Guntur, Andhra Pradesh
INDIA
sharmilad@gmail.com
ORCID 0000 0002 9121 0702

Rao M. C.
Department of Physics,
Andhra Loyola College, Vijayawada,
Andhra Pradesh,
India
raomc72@gmail.com
ORCID 0000-0001-9136-9679

Naveen Kumar. V
Department of Basic Sciences and
Humanities, Seshadri Rao Gudlavalleru
Engineering College, Gudlavalleru,
Andhra Pradesh,
India
vnkbjs@gmail.com
ORCID 0000-0002-3838-6733

Krishna Jyothi. N
Department of Physics, Sri Sathya Sai
University for Human Excellence,
Kalaburagi, Karnataka,
India
jyothinadella82@gmail.com
ORCID 0000-0003-0721-0695